

Supporting Information for:

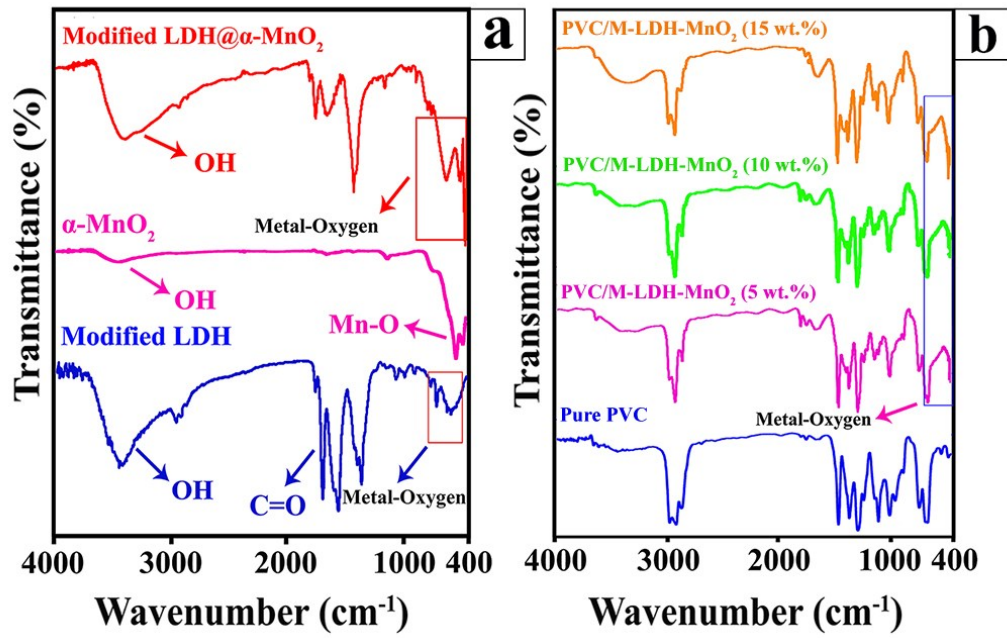
Design and identification of poly(vinyl chloride)/layered double hydroxide@MnO₂ nanocomposite films and evaluation of methyl orange uptake: Linear and non-linear isotherm and kinetic adsorption models

Shadpour Mallakpour * , Mina Naghdi

Organic Polymer Chemistry Research Laboratory, Department of Chemistry, Isfahan University of Technology, Isfahan, 84156-83111, Islamic Republic of Iran

* Corresponding author at. Organic Polymer Chemistry Research Laboratory, Department of Chemistry, Isfahan University of Technology, Isfahan, 84156-83111, I. R. Iran.

E-mail address: mallak@jut.ac.ir, mallak777@yahoo.com (S. Mallakpour).



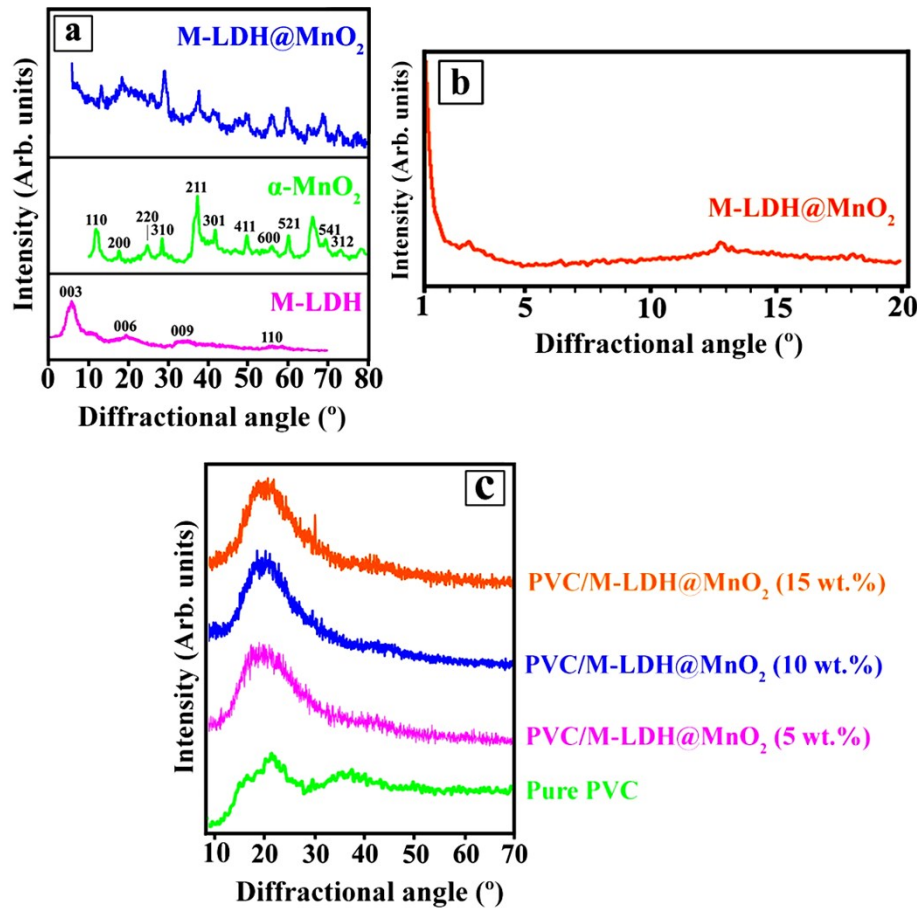


Figure S2 (a) XRD patterns of the M-LDH, α -MnO₂ nano-rods, and M-LDH@MnO₂ hybrid nano-filler, (b) low angle XRD of the M-LDH@MnO₂ hybrid nano-filler, (c) XRD patterns of pure PVC, and PVC/M-LDH@MnO₂ nanocomposite films (5, 10, and 15 wt.%).

Table S1 Atomic percentages from EDX spectra of α -MnO₂ nano-rods, M-LDH, M-LDH@MnO₂ hybrid nano-filler, and PVC/M-LDH@MnO₂ nanocomposite 15 wt.%.

Sample	Atomic percentage							
	K	Mn	Mg	Al	O	N	C	Cl
α -MnO ₂ nano-rods	7.2	46.45	-	-	46.35	-	-	-
M-LDH	-	-	5.70	3.26	52.44	15.87	22.73	-
M-LDH@MnO ₂ hybrid nano-filler	1.17	6.51	3.73	1.88	56.05	7.56	23.1	-
PVC/M-LDH@MnO ₂ nanocomposite 15 wt.%	-	0.55	0.50	0.22	5.04	3.89	65.33	24.27

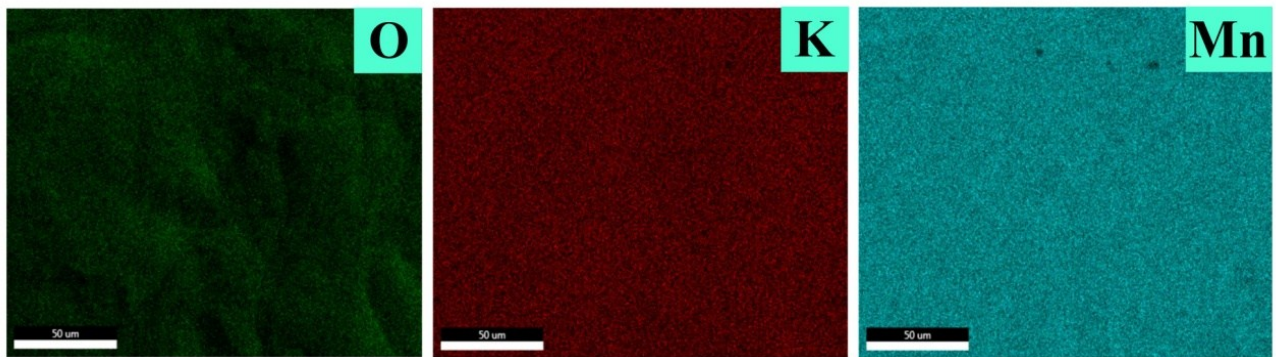


Figure S3 Mapping of α -MnO₂ nano-rods.

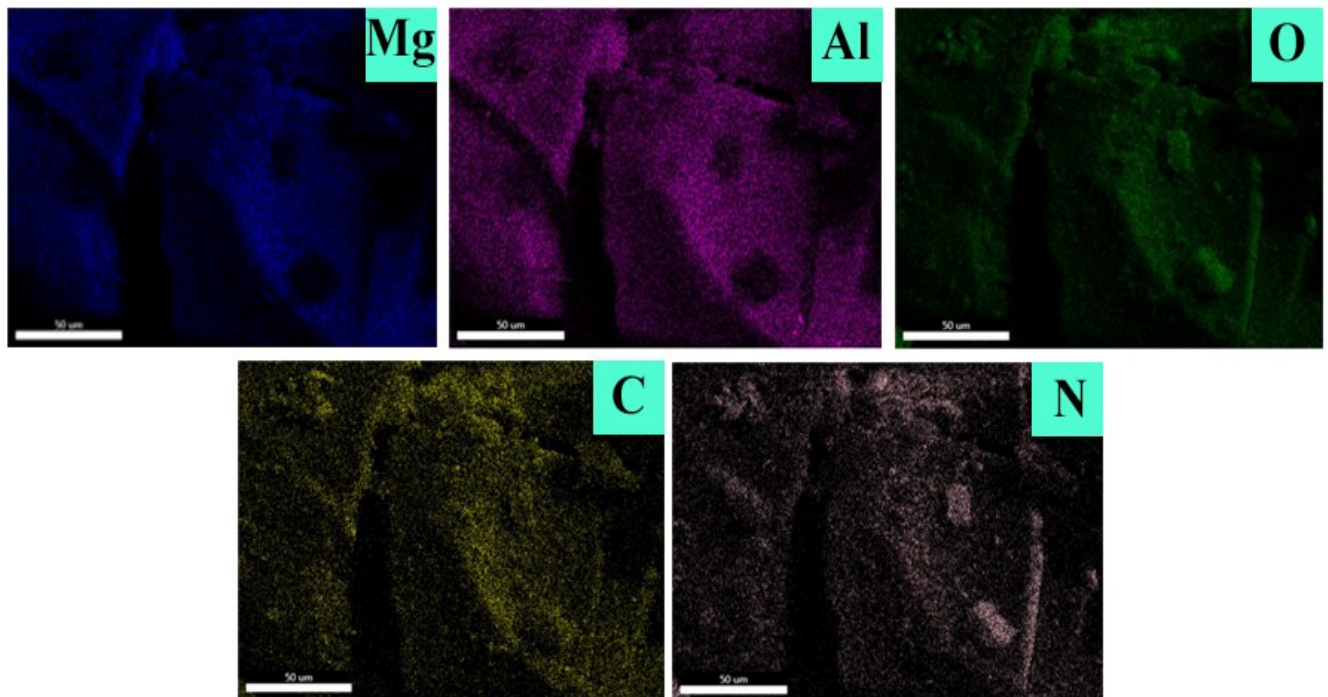


Figure S4 Mapping of M-LDH.

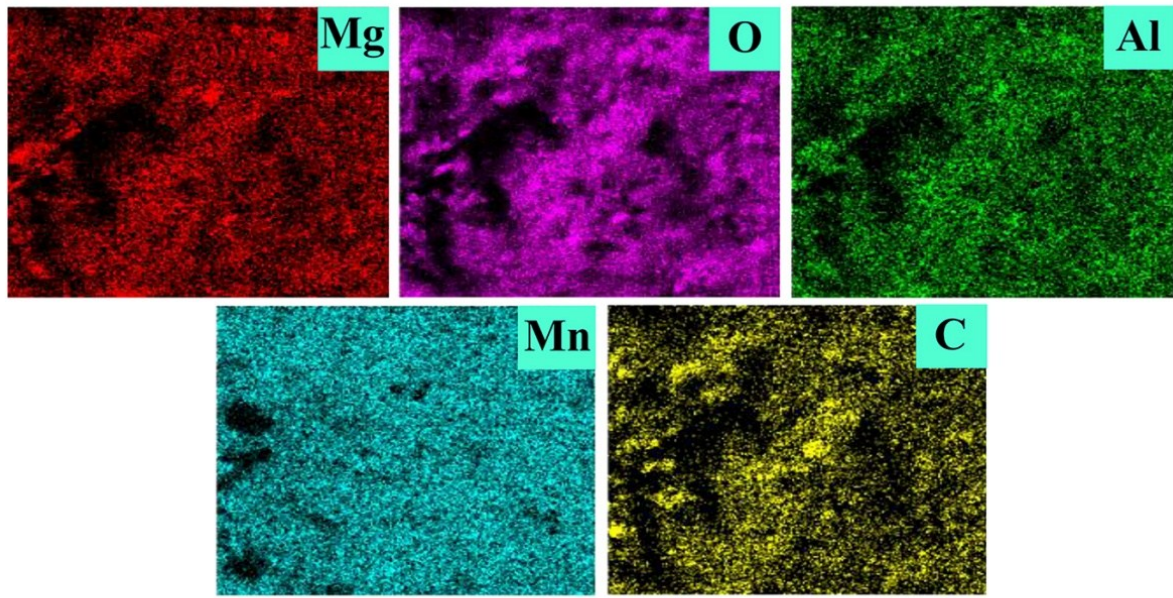


Figure S5 Mapping of M-LDH@MnO₂ hybrid nano-filler.

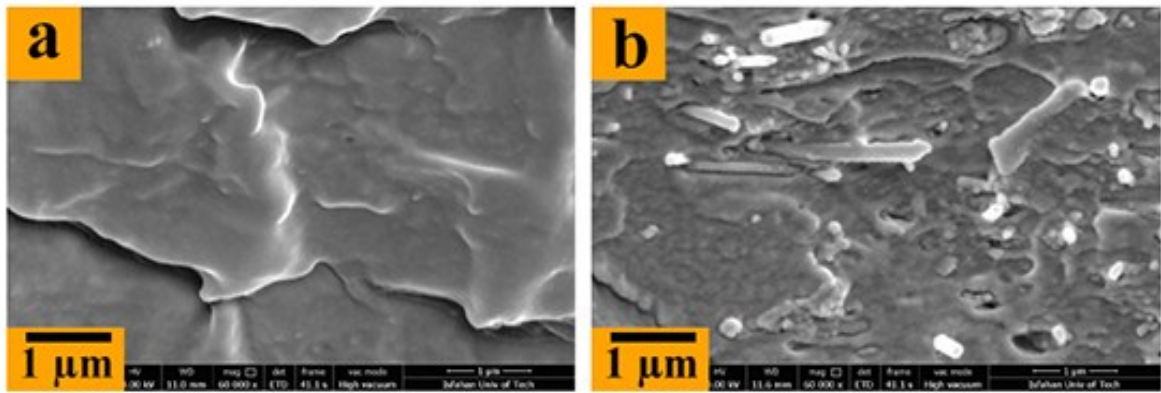


Figure S6 Cross-sectional FESEM images of the (a) PVC and (b) PVC/M-LDH@MnO₂ nanocomposite 10 wt.%.

Table S2 Pore structural information for the M-LDH, M-LDH@MnO₂ hybrid nano-filler, and PVC/M-LDH@MnO₂ nanocomposite 15 wt.%.

Sample	Mean pore diameter (nm)	Total pore volume (cm ³ /g)	Reference
M-LDH	38.86	0.007	1
M-LDH@MnO ₂ hybrid nano-filler	32.35	0.222	This work
PVC/M-LDH@MnO ₂ nanocomposite 15 wt.%	34.95	0.224	This work

Table S3 Char yield values for the α-MnO₂ nano-rods, M-LDH, and M-LDH@MnO₂ hybrid nano-filler.

Sample	Char yield (%) ^a	Reference
α-MnO ₂ nano-rods	92	2
M-LDH	44	1
M-LDH@MnO ₂ hybrid nano-filler	59	This work

^a Weight (%) of undecomposed sample after heating at 800 °C.

Table S4 Equations for the isotherm, kinetic, Intraparticle, and liquid film diffusion models.

Model	Linear
Langmuir (linear form)	$C_e Q_e = 1/(Q_m K_L) + C_e/Q_m$
Langmuir (non-linear form)	$Q_e = (Q_m \times C_e \times K_L)/(1 + C_e K_L)$
Freundlich (linear form)	$\ln Q_e = \ln K_F + 1/n \ln C_e$
Freundlich (non-linear form)	$Q_e = K_F \times C_e^{1/n}$
Pseudo-first order (linear form)	$\ln (Q_e - Q_t) = \ln Q_e - k_1 t$
Pseudo-first order (non-linear form)	$Q_t = Q_e [1 - \exp(-k_1 t)]$
Pseudo-second order (linear form)	$t/Q_t = 1/k_2 Q_e^2 + t/Q_e$
Pseudo-second order (non-linear form)	$Q_t = Q_e^2 k_2 t / (1 + Q_e k_2 t)$
Weber's intraparticle diffusion	$Q_t = k_{ip} t^{0.5} + C$
Liquid film diffusion	$\ln (1-F) = k_{fd} \cdot t$

Table S5 r^2 and errors' mathematical equations.

Parameters	Relationships
r^2	$\frac{\sum_{i=1}^n (y_{exp} - \bar{y}_{cal})^2}{\sum_{i=1}^n (y_{exp} - \bar{y}_{cal})^2 + \sum_{i=1}^n (y_{exp} - y_{cal})^2}$
RMSE	$\sqrt{\frac{1}{n} \sum_{i=1}^n (y_{exp} - y_{cal})^2}$
χ^2	$\sum_{i=1}^n \frac{(y_{exp} - y_{cal})^2}{y_{cal}}$
SSE	$\sum_{i=1}^n (y_{exp} - y_{cal})^2$

References

1. S. Mallakpour and M. Hatami, *Appl. Clay Sci.*, 2017, **149**, 28-40.
2. S. Mallakpour, A. Abdolmaleki and H. Tabebordbar, *Europ. Polym. J.*, 2016, **78**, 141-152.